RESULTS OF OBSERVATION CAMPAIGNS FOR SATELLITE ORBITAL AND ATTITUDE MOTION DETERMINATION

Fabio Santoni(1), Fabrizio Piergentili(2)

(1) DIAEE, University of Rome "La Sapienza", Via Eudossiana 18, 00184 – Rome (Italy), fabio.santoni@uniroma1.it
(2) DIMA, University of Rome "La Sapienza", Via Eudossiana 18, 00184 – Rome (Italy), fabrizio.piergentili@uniroma1.it

ABSTRACT

The results of observation campaigns conducted in the last years by the Aerospace Systems Laboratory at Università di Roma "La Sapienza" are summarized in this paper. These mainly refer to orbital determination of objects in the GEO region, analyzing in particular close approach events, and to measurements of the attitude motion status of disposed upper stages and satellites in LEO.

1 INTRODUCTION

The Aerospace Systems Laboratory at Università di Roma "La Sapienza" was established in 2010 and it is mainly involved in satellite subsystems design and realization and in space debris observation. The team gained experience in these fields, participating in the design and realization of the first satellites of the UNISAT program at Scuola di Ingegneria Aerospaziale [1-6] and being involved in the first space debris observation and mitigation activities developed in Italy [7-10]. The activities being currently carried on in the field of space systems include the development of highly integrated and innovative on-board components and techniques, such as miniaturized attitude control systems, plastics nanosatellite structures, studies on nanosatellite laser propulsion [11-13]. The activities being currently carried on in the field of space debris include theoretical studies on collision probability in multiple nanosatellite launches, and optical observation campaigns [14-16].

These optical observation campaigns are based both on commercial hardware and on specifically developed optical systems, as described in section 2. The activities

2 OPTICAL OBSERVATION SYSTEM

The optical observation system used in the observation campaigns depicted in this paper consists mainly of five parts: the telescope, the mount, the CCD or a camera, a precise timing unit based on a GPS receiver and a computer that controls the whole system.

2.1 Telescope

The optical part of the system is the telescope, designed to take as much light as possible, based on a Rila® optical configuration, and focuses it on a CCD sensor. Its focal length limits the width of the field of view (FOV) that has to be large enough to allow the matching of stars visible in the picture with a stellar catalogue in order to evaluate magnitude and to perform astrometric measurements. The telescope used is shown in figure 1. It is a modified Cassegrain design reflector telescope, with a 25 centimetres main mirror diameter, and 750 millimetres of focal length, obtaining a focal ratio equal to f/3. These characteristics ensure a good trade off in term of resolution and FOV size. In addition, compactness and relatively low cost are characteristics of this system.

Figure 1. The telescope used for optical measurements

2.2 Mount

The mount is a Skywatcher NEQ 6-PRO with SynScan Hand Control, with 0.144 arcsec stepper motor resolution and slewing speed up to 3.4 degrees per second (800x), shown in figure 2. It is a German Equatorial Mount, which is characterized by a T-shape primary structure where the telescope is placed on one end of the upper bar (Declination) while on the other end suitable counterweight are necessary. The lower bar of the T-shape structure is the right ascension axis.

Proc. '6th European Conference on Space Debris'
Darmstadt, Germany, 22–25 April 2013 (ESA SP-723, August 2013)

Figure 2. Mount used for optical observations

2.3 Sensor

A DTA Discovery Plus DX-3200 E CCD camera, shown in figure 3, has been used. It is equipped with a Kaf-3200 E sensor, obtaining a resolution of 2184x1472 pixels, a viewing area of 14.64x10.26 mm and a pixel size of 6.8x6.8 micrometres. This CCD camera is also equipped with an external trigger system, which permit to the user to open the shutter only when a particular external electric signal is sent to the camera, in order to obtain a precise exposure timing.

Figure 3. CCD camera used for the optical observations campaign

2.4 Timing unit

In order to achieve good results in attitude determination, the need for a certain level of timing measurement accuracy is required. Thus, it is necessary to know both the precise instant in which the measure is acquired, and have the certainty that the shutter of the CCD is open precisely at the same instant of time reported in the header of photo. To meet these needs, the system was equipped with a GPS receiver connected both to the computer that manages the entire system, and to the external trigger control of the CCD. The connection to the computer is used to synchronize the time with the UTC time, while to the trigger door of the CCD is sent a voltage signal with a frequency of one Hertz, commonly called Pulse Per Second (PPS), which is used to control the shutter opening. During the observation campaign a customized GPS receiver has been used (it is shown in figure 4).

Figure 4. GPS receiver used for the observation campaign

2.5 Control system

The last component of the system is the computer that controls, interface and automates the rest of the system. In particular, using appropriate software, the computer is able to interface with the GPS receivers, to command the mount, and to control the CCD that captures the images. Also, the computer has the function to store the data in the expectation that they are analyzed and has the function to fill in the header of the captured images, by entering all the parameters needed for subsequent operations, including: angular position of the center of the picture, time of exposure start, exposure duration, temperature of CCD, type of binning used and number of pixels. The complete functional scheme of the observation system is sketched in Figure 5.

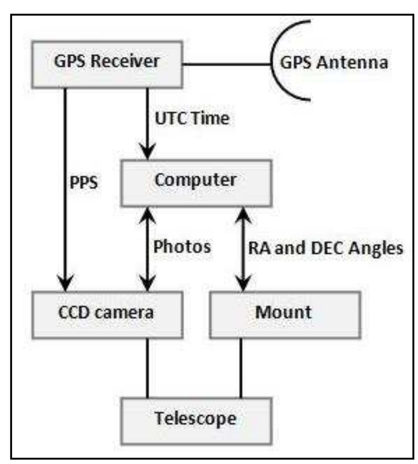

Figure 5. Optical system functional scheme

3 OBSERVATION CAMPAIGNS STATISTICS

During the observation campaign, 21 nights of observations were conducted in a time span of about 9 months. A total of 12975 pictures were taken, for a total of 86.1 hours of observation. During these acquisitions, satellites from different orbital regimes were photographed, including LEO, MEO and GTO. The activity focussed mainly on rocket bodies, with the aim to study their attitude tumbling or stabilized motion, and on GEO satellites, in particular the Italian satellites SICRAL-1 and SICRAL-1B.

In Figures 6 and 7 the number of pictures and the total observation time per night are reported, for the different orbital regimes and object tracked. The first nights have been devoted mainly to the system calibration, acquiring many pictures of GPS satellites, to compare with their very accurate and publicly available ephemerides.

The percentage of pictures taken and time per satellite typology are sketched in Figures 8 and 9.

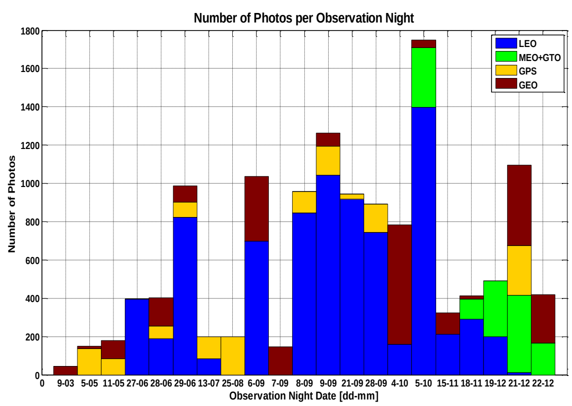

Figure 6. Number of Pictures taken per observation night.

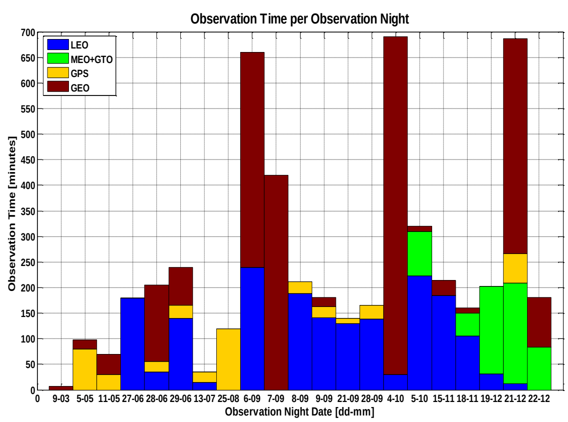

Figure 7. Observation time per observation night.

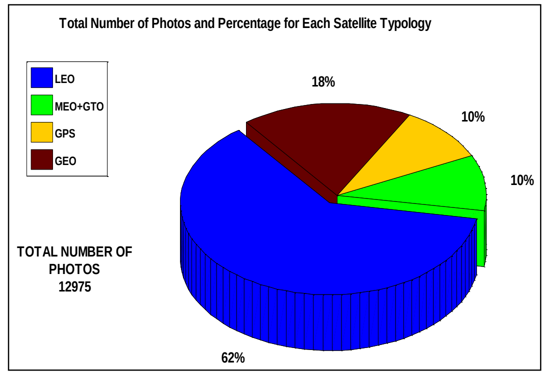

Figure 8. Number of pictures per orbital regime.

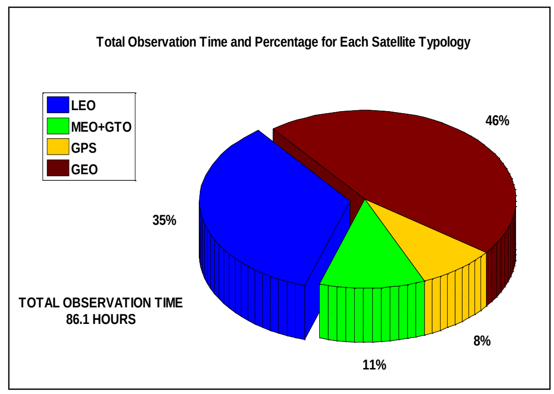

Figure 9. Observation time per orbital regime.

4 RESULTS IN ORBIT DETERMINATION

Starting from the data achieved from observation campaigns previously depicted, Orbit Determinations were performed, considering different sampling frequency and observation time spans. One of the objectives of the study was to obtain a comparison between optical orbit determination and TLE propagation. The angular measures residuals were analysed in both cases, inferring the quality of the estimation. In addition, information on the state covariance was obtained and compared to the TLEs one.

The first Orbit Determination process was performed using the optical measurements of the Italian GEO satellite SICRAL 1-B, obtained in the two consecutive nights of August 1st and 2^{nd}. In the first day few measures were obtained, in a thirty minutes time span, while in the second day 148 measures were obtained in a three hours time span. In both cases the acquisition frequency was about one picture per minute. This measure time span is not sufficient to obtain accurate results. However, two Orbit Determinations were performed using these measurements set; the first one based on the measures of the second day only, the second one on the measures from both days.

The state estimated at the instant of the first measure for the first OD is presented here below, where the corresponding values obtained from the TLE are also shown.

$$\overrightarrow{x_{EST}} \left\{ \begin{array}{ll} 10843.770545 & \text{km} \\ -40721.143137 & \text{km} \\ -27.939919 & \text{km} \\ 2.970598 & \text{km/s} \\ 0.790026 & \text{km/s} \\ -0.008466 & \text{km/s} \end{array} \right. \qquad \overrightarrow{x_{TLE}} \left\{ \begin{array}{ll} 10862.828569 & \text{km} \\ -40736.326646 & \text{km} \\ -28.541045 & \text{km} \\ 2.971089 & \text{km/s} \\ 0.792635 & \text{km/s} \\ -0.008607 & \text{km/s} \end{array} \right.$$

$$|\overrightarrow{r_{EST}}| = 42139.980559 \text{ km} \qquad |\overrightarrow{r_{TLE}}| = 42159.817091 \text{ km}$$

We observe a quite high difference, of about 20 kilometres, between the two position magnitudes. This result is due to the slow convergence of the estimation process based on angular measurements only, which needs for several hours of observation in order to accurately estimate the satellite range, while the orbital plane is immediately accurately estimated. These results are also evident by analysing the estimated osculating orbital parameters, shown in table 2. The semimajor axis is too small and the eccentricity too high for a controlled geostationary satellite, confirming the difficulty in the orbit shape determination with only few hours of observation. The poor quality of the estimation is also confirmed by the residuals analysis. By propagating the estimated state to the instants of the measures of the day before, an error of 3650 arcsec was obtained along track, while only 6.9 arcsec was obtained off-track, against the 66 arcsec and 4.1 arcsec respectively obtained by considering the specific TLE. Again these results confirms that by considering only three hours of measures the orbital plane is well estimated, while the orbit shape is not accurately determined. The residuals on the measures used for the Orbit Determination are shown in figure 10, obtaining a mean value of 6.12”. This confirms that the poor estimation quality is due to the short time period and not to the quality of the measurements.

Semimajor Axis (a) [km]	42094.131
Eccentricity (e) [\]	1.120e-3
Inclination (i) [deg]	0.162
RAAN (Ω) [deg]	91.375
Argument Of Perigee (ω) [deg]	28.967

Table 2. August 2nd Orbit Determination: Orbital Parameters

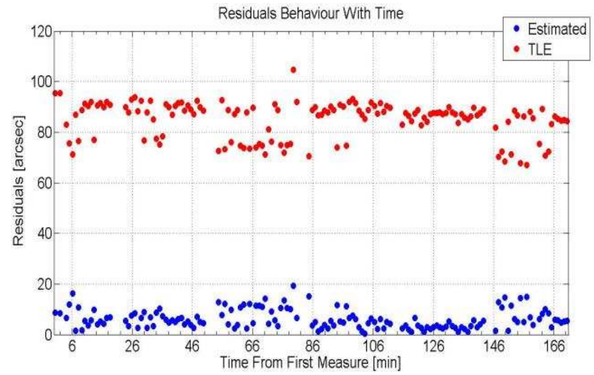

Figure 10. August 2nd Orbit Determination: Residuals

By considering also measures obtained about 24 hours before the first measure of August 2nd, for a total time span of abut 27 hours between the first and the last measure, the state estimation quality increases considerably. This is evident in the comparison between the estimated state and the one obtained by the TLE, presented below. In particular the determined position magnitude is close to the one obtained by TLEs.

$$\overrightarrow{x_{EST}} \left\{ \begin{array}{ll} 11150.233347 & \text{km} \\ -40657.006293 & \text{km} \\ -31.247788 & \text{km} \\ 2.965463 & \text{km/s} \\ 0.813822 & \text{km/s} \\ -0.008444 & \text{km/s} \end{array} \right. \qquad \overrightarrow{x_{TLE}} \left\{ \begin{array}{ll} 11162.501752 & \text{km} \\ -40655.289453 & \text{km} \\ -30.123238 & \text{km} \\ 2.965173 & \text{km/s} \\ 0.814488 & \text{km/s} \\ -0.008526 & \text{km/s} \end{array} \right.$$

$$|\overrightarrow{r_{EST}}| = 42158.283294 \text{ km} \qquad |\overrightarrow{r_{TLE}}| = 42159.873372 \text{ km}$$

In this case, the determined osculating orbital parameters, presented in table 3, confirm the higher quality of estimation. In particular the obtained semimajor axis and eccentricity are typical of geostationary satellites, confirming that a two days time distance between the first and the last measure, even if the measures are not obtained continuously during the time span, increases the estimation quality considerably, in particular in terms of orbit shape. The orbit plane parameters, , are similar to the one obtained with only three hours of measures, confirming that the orbital plane is easier to estimate than the orbit shape. The residuals analysis depicted in figure 11, where the residuals between the measures and the estimated angular position and the measures and the angular position obtained from the TLE are shown. A mean value of 6.18 arcsec has been obtained for the estimated residuals. After a propagation of more than 24 hours, the residuals are not increased as in the previous case, remaining lower that 10 arcseconds. This confirms the quality of the estimation and the improvement with respect to the Orbit Determination performed by using a three hour time span measurement set.

Semimajor Axis (*a*) [km]	42164.957
Eccentricity (*e*) [\]	2.300e-4
Inclination (*i*) [deg]	0.163
RAAN (*Ω*) [deg]	90.231
Argument Of Perigee (*ω*) [deg]	118.3128

Table 3. August 1st & 2nd Orbit Determination: Orbital Parameters

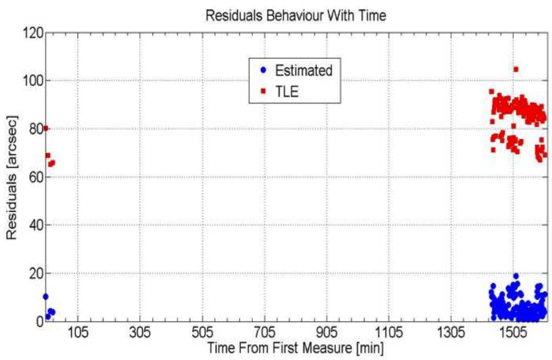

Figure 11. August 1st & 2nd Orbit Determination: Residuals

A mean value of 6.18 arcsec has been obtained for the estimated residuals. After a propagation of more than 24 hours, the residuals are not increased as in the previous case, remaining lower that 10 arcseconds. This confirms the quality of the estimation and the improvement with respect to the Orbit Determination performed by using a three hour time span measurement set.

In all the cases presented, the real satellite position was verified to be within the estimated 3-sigma position covariance shell during all the propagation time span, so the small covariance ellipsoids obtained can be considered truthful and trustworthy, even if they are much smaller than the one obtained by the TLEs. This means that by using the Orbit Determination method presented in this work, much more trustworthy collision probabilities with respect to the one obtained by considering the TLEs can be calculated, being the estimations much accurate and the covariance ellipsoids smaller. Typical results of covariance achieved are resumed in table 4 and table 5, where the Along-Track and the Position Errors Standard Deviations are shown.

The optical system used in this work reaches a measurement error Standard Deviation of about 3.5 arcsec, both in Right Ascension and Declination, and negligible measurement biases. By using a batch Non-Linear Least Squares filter, accurate Orbit determinations have been performed the main results obtained can be summarized as follows:

a) Using data from a single observation night, corresponding to about one third of the orbit in GEO, the orbital period cannot be evaluated very accurately. Propagating the estimated state for the 48 hours following the OD epoch, a position error comparable with the TLEs is obtained (around 10-15 km).

b) Using data from a single night and a short time (less than one hour) in the following night, the accuracy improves drastically, reducing the position error below one kilometre and obtaining position covariance 3σ ellipsoid dimensions lower than 2 km.

c) Based on the results in b), the true collision probability can be evaluated.

Along-Track Error Standard Deviation				
	24 Hours Propagation	36 Hours Propagation	48 Hours Propagation	Maximum Value
One Night Measurements Covariance	10.14 km	12.24 km	20.42 km	20.42 km
Two Nights Measurements Covariance	0.21 km	0.52 km	0.49 km	0.72 km
TLE Covariance	5.99 km	6.92 km	6.40 km	7.02 km

Table 4. Along-Track Error Standard Deviation Comparison

Position Error Standard Deviation				
	24 Hours Propagation	36 Hours Propagation	48 Hours Propagation	Maximum Value
One Night Measurements Covariance	10.17 km	12.34 km	20.43 km	20.43 km
Two Nights Measurements Covariance	0.31 km	0.55 km	0.54 km	0.73 km
TLE Covariance	6.00 km	6.93 km	6.41 km	7.03 km

Table 5. Position Error Standard Deviation Comparison

5 RESULTS IN LIGHT CURVE ANALYSIS

The image analysis provides the photometric signatures of the orbiting objects, which as mentioned previously, will be used for the attitude determination. An appropriate, friendly user, software for photometric analysis and calibration was developed and tested in MatLab®. It allows, once the photo is loaded, to extrapolate the light curve related to the satellite.

The program for extrapolation of the light curves can be summarized by the following steps:

- Uploading of photos on MatLab®, from which information about the time instant of the photo and the exposure time are taken, and then the image is plotted to allow the next steps;
- Determination of observer position;
- Uploading of TLE, it is inserted in order to calculate the position of the satellite, which is useful to determine the phase angle (crucial in the algorithm for the attitude determination), and for the calculation of the angular velocity of satellite with respect to the observer;
- Selection of a dark portion of the sky, or rather a portion of sky where there are not stars or visible objects; which will be used to calculate the sky background and to determine the effective flux due to the stars or the satellite;
- Selection of the reference stars whose brightness is known through the use of the astrometry software previously employed;
- Selection of the satellite strip from which the light curve is extrapolated.

A snapshot of the process just described is shown in figure 12.

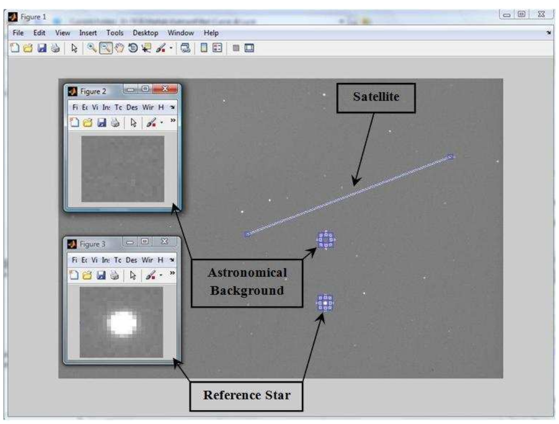

Figure 12 Example of image analysis software.

The code developed is able to provide the value of the brightness of the satellite at any point of the strip, assigning to each point the related time instant. Furthermore, the algorithm implemented is able to evaluate the brightness even if the strip is not complete, in this case the difficulty arises from being able to assign at the brightness value the related time instant; for this purpose it was calculated the angular velocity of the satellite with respect to the observer. This feature is especially useful for LEO satellites which, because of their speed and the relatively small field of view, in the span of only 10 to 15 seconds can pass through it completely.

For satellites with rotation periods longer than the exposure time, it is impossible to acquire in the same picture a maximum and a minimum value of brightness. Hence, in order to use and compare data from more than one picture, a normalization of the brightness with respect both to the distance from the observer and the phase angle, was implemented.

An example of a picture and the related light curve, obtained for the satellite SL-26 RB Norad Code 37399, is shown in figures 13 and 14. The rapid changes in brightness are evident in Fig.13 and 14, from which it is possible to infer that the depicted rocket body is tumbling.

Figure 13 Example of tumbling orbiting object.

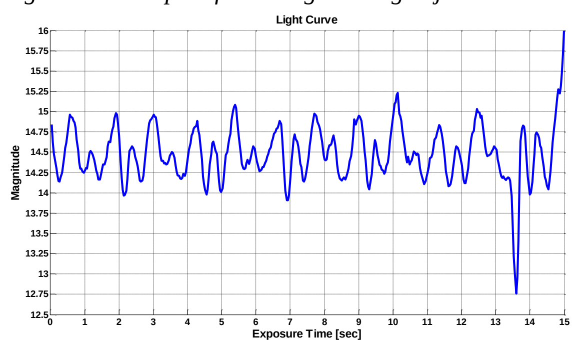

Figure 14. Light curve of the body in Fig. 13.

An example of light curve for ENVISAT is shown in fig. 15. Apparently the attitude is stable, or at least changing over much longer time periods than the exposure time.

Figure 13 Example of attitude stable object (ENVISAT).

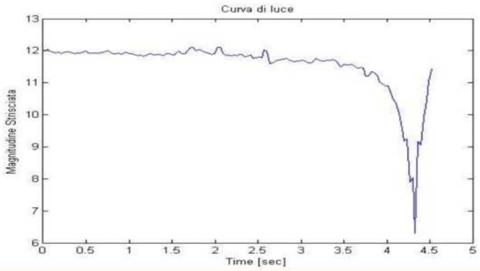

Figure 14. Light curve of the body in Fig. 13.

6 CONCLUSIONS

The results of observation campaigns carried on in the last years at the Aerospaxe Systems Laboratory of University of Rome "La Sapienza" have been described, including details on the hardware used. Experimental activity was conducted mainly in close approach analysis in the GEO region and in rotational status of disposed upper stages.

REFERENCES

1. Santoni F., "Risk Management for Microsatellite Design", Acta Astronautica, Volume: 54, Issue: 3, February 2004, p.221–228, doi: 10.1016/S0094-5765(02)00291-6.

2. Santoni, F., Ferrante, M., Graziani, F., Ferrazza, F., "In orbit performance of the UNISAT terrestrial technology solar panels", 2001 IEEE Aerospace Conference Proceedings, Big Sky, MT, 10-17 March 2001, Volume 1, 2001, pp.1363-1371.

3. Santoni, F. , Piergentili, F., Bulgarelli, F. , Graziani, F., "UNISAT-3 power system", ESA SP-589, Seventh European Space Power Conference, 9-13 May 2005, Stresa, Italy, pp. 395-400.

4. Santoni, F., Zelli, M., "Passive magnetic attitude stabilization of the UNISAT-4 microsatellite", Acta Astronautica, vol. 65, September-October 2009, p. 792-803, doi: 10.1016/j.actaastro.2009.03.012

5. Santoni, F., Piergentili, F., Graziani, F., "In orbit performances of the UNISAT-3 solar arrays", Proc. of the 57th International Astronautical Congress, IAC 2006, Valencia, Spain, 2-6 October 2006, Volume 9, Pages 5920-5926.

6. F. Graziani, F. Piergentili, F. Santoni, "A space standards application to university-class microsatellites: the UNISAT experience", Acta Astronautica, vol. 66, Issues 9-10, May-June 2010, p. 1534-1543, doi: 10.1016/j.actaastro.2009.11.020

7. M. Porfilio, F.Piergentili, F. Graziani. 'First optical space debris detection campaign in Italy', Advances In Space Research. vol. 34, pp. 921 – 926; doi: 10.1016/j.asr.2003.02.035

8. M. Porfilio, Piergentili F., F. Graziani, Two-site orbit determination: The 2003 GEO observation campaign from Collepardo and Mallorca, Advances In Space Research. vol. 38, pp. 2084 – 2092, doi:10.1016/j.asr.2006.06.004,

9. M. Porfilio, F. Piergentili, F. Graziani, "The 2002 italian optical observations of the geosynchronous region", Spaceflight Mechanics 2003, Advances In The Astronautical Sciences, vol. 114, American Astronautical Society, San Diego, USA, 2003 AAS paper n. AAS 03-186, ISBN:0-87703-504-0.

10. F. Piergentili, F. Graziani, "SIRDARIA: A low-cost autonomous deorbiting system for microsatellites", paper IAC-06-B6.4, 57th IAC, International Astronautical Congress 2006, Valencia, Spain, 2-6 October 2006.

11. Candini G.P., Piergentili F., Santoni F., "Miniaturized attitude control system for nanosatellites", Acta Astronautica, Volume 81, Issue 1, December 2012, p.325-334. doi: 10.1016/j.actaastro.2012.07.027.

12. Piattoni, J., Candini, G.P., Pezzi, G., Santoni, F., Piergentili, F., "Plastic Cubesat: An innovative and low-cost way to perform applied space research and hands-on education", Acta Astronautica, Vol.81, Issue 2, December 2012, pp.419-429. doi: 10.1016/j.actaastro.201207.030.

13. L. Felicetti, F. Santoni, "Nanosatellite swarm missions in low Earth orbit using laser propulsion", Aerospace Science and Technology, (July 2013), doi: 10.1016/j.ast.2012.08.005.

14. F. Santoni, F. Piergentili, F. Graziani, "Broglio Drag Balance for neutral thermosphere density measurement on UNICubeSAT", Advances in Space Research, vol. 45, Issue 5, 2010, p. 651-660, ISSN: 0273-1177, doi: 10.1016/j.asr.2009.10.001.

15. Santoni, F., Piergentili,F., Ravaglia, R., "Nanosatellite Cluster Launch Collision Analysis", Journal of Aerospace Engineering, Vol. 26, No. 3, 2013, doi: 10.1061/(ASCE)AS.1943-5525.0000175.

16. F.Santoni, R. Ravaglia, F. Piergentili, "Analysis Of Close Approach In GEO Using Optical Measurements", paper IAC-12,A6,5,22.p1,x14304, 63rd International Astronautical Congress, Naples, Italy, 1-5 October 2012.

17. F. Santoni, E. Cordelli, F.Piergentili, "Determination of Disposed-Upper-Stage Attitude Motion by Ground-Based Optical Observations", Journal of Spacecraft and Rockets, Vol. 50, 2013, doi:10.2514/1.A32372.